https://doi.org/10.5194/tc-2021-144
Preprint. Discussion started: 25 May 2021

The Cryosphere Discussions

Brief communication: lack of agreement in remote sensing detection of cyclonic drift caused by Atlantic weather in Antarctic sea ice

Wayne de Jager[1], Marcello Vichi[1,2]

[1]Department of Oceanography, University of Cape Town, Cape Town, 7700, South Africa
[2]Marine and Antarctic Research Centre for Innovation and Sustainability (MARIS), University of Cape Town, Cape Town, 7700, South Africa

Correspondence to: Wayne de Jager (djgway001@myuct.ac.za)

Abstract. Sea-ice extent variability, a measure based on satellite-derived sea ice concentration measurements, has traditionally been used as an essential climate variable to evaluate the impact of climate change on polar regions. However, concentration-based measurements of ice variability do not allow to discriminate the relative contributions made by thermodynamic and dynamic processes, prompting the need to use sea-ice drift products and develop alternative methods to quantify changes in sea ice dynamics that would indicate trends in Antarctic ice characteristics. Here, we present a new method to automate the detection of rotational drift features in Antarctic sea ice at daily timescales using currently available remote sensing ice motion products from EUMETSAT OSI SAF. Results show that there is a large discrepancy in the detection of cyclonic drift features between products, both in terms of intensity and year-to-year distributions, thus diminishing the confidence at which ice drift variability can be further analysed. Product comparisons showed that there was good agreement in detecting anticyclonic drift, and cyclonic drift features were measured to be 1.5-2.2 times more intense than anticyclonic features. The most intense features were detected by the merged product, suggesting that the processing chain used for this product could be injecting additional rotational momentum into the resultant drift vectors. We conclude that it is therefore necessary to better understand why the products lack agreement before further trend analysis of these drift features and their climatic significance can be assessed.

1 Introduction

The Antarctic continent is surrounded by seasonally varying sea ice. During the austral winter, sea ice coverage expands zonally when progressing northward into the Southern Ocean, and conversely constricts south towards Antarctica's coastline in the austral summer. Sea ice plays a major role in ocean and atmosphere interactions, primarily acting as a heat, mass and momentum exchange modulator between the surface water and overlying air masses (McPhee et al., 1987; Vihma et al., 2014). Sea ice coverage is a key component of the Southern Ocean climate system and therefore also the global climate system (Mayewski et al., 2009). Antarctic sea ice is characterized by its high temporal and spatial variability (Parkinson, 2019), and thus it is necessary to define and measure this variability for future trend analysis. Due to the difficulties associated with accessing the polar regions, *in situ* measurements of sea ice properties are both scarce and sparse. The detection of sea ice via remote sensing techniques is therefore a critical component of mapping its distribution. Reliable satellite derived sea ice

https://doi.org/10.5194/tc-2021-144
Preprint. Discussion started: 25 May 2021

distribution estimates date back to 1978 (Turner et al., 2016), datasets which are now fundamental to our understanding of sea ice variability and the backbone of polar climatological analysis.

Traditionally, sea ice concentration (SIC, a measure of the proportion of ice-covered water to water not covered by ice) has been derived from the passive microwave (PM) brightness temperature of the ocean surface and used to estimate the location of the ice edge and infer the sea ice extent (SIE, a measure of the area of ocean surface covered by 15 % or greater SIC). Trends in SIE are commonly used indicators of sea ice variability in both the Arctic and Antarctic regions, and subsequently presented to highlight the effects of global warming. Antarctic SIE is characterized by its dramatic variability with regionally distinct trends, with a record high SIE measured in 2014 and record low measured in 2017 (Parkinson, 2019). It is, however, noteworthy that SIE only considers the area of SIC greater than 15 %, and not any changes within the 15 % - 100 % range. Furthermore, the decision to define a lower threshold of 15 % in the definition of SIE is one of traditional convention based on the radiometric properties of sea ice relative to that of open water, rather than one based on any dynamic or thermodynamic considerations (Comiso and Zwally, 1984). This highlights a limitation of using the SIE as a metric of ice variability - particularly when attempting to forecast or hindcast sea ice coverage in models (Notz and Community, 2020). This limitation could potentially be exacerbated in the Southern Ocean. Unlike in the Arctic basin, Antarctic sea ice is unbounded by land, resulting in a far more dispersive and non-uniform growth pattern during the freezing months, and frequent cyclone passages and intense wave induced break up alters the ice landscape far into the ice interior (Kohout et al., 2014; Uotila et al., 2011). Additionally, the weakly stratified upper ocean in the Antarctic results in a considerably higher ocean-to-atmosphere heat flux, thus limiting the growth of sea ice on the ocean surface (Martinson and Iannuzzi, 2013).

While temporal variability in SIC can be computed from PM data, identifying the mechanisms driving this variability is less obvious. Dynamic and thermodynamic processes together alter the Southern Ocean's ice landscape (Stevens and Heil, 2011), however, concentration-only based measurements from space do not allow to discriminate their relative contributions. Ice motion products can therefore be used in conjunction with ice concentration products to help distinguish the dynamical component. These products use a feature tracking method, whereby a distinguishable pattern in the ice is identified and followed across a temporal sequence of brightness temperature (or backscatter) maps. Momentum exchange from the overlying atmosphere and the ocean surface primarily drive ice movement, while waves, ocean tilt, Coriolis forcing, ice inertia and internal ice stressors also play a role (Feltham, 2008). Winter sea ice cover in the Southern Ocean limits ocean surface current data acquisition, thus ocean-to-ice momentum exchange is not well understood. Seasonal patterns and long-term trends in Southern Ocean sea ice drift have shown a strong correlation with local winds (Holland and Kwok, 2012). Satellite derived drift speeds between 1982-2015 were measured to be ~1.4 % of the geostrophic wind, while Arctic sea ice drift speed was approximately half of that over the same period, suggesting that Antarctic sea ice is more susceptible to wind forcing (Kwok et al., 2017). Furthermore, the El Nino Southern Oscillation (ENSO) and the Southern Annular Mode (SAM) have also been

https://doi.org/10.5194/tc-2021-144
Preprint. Discussion started: 25 May 2021

shown to influence sea ice variability (Goosse et al., 2009; Pezza et al., 2012; Thompson, 2002; Yuan, 2004). However, the degree of relative influence of these larger scale atmospheric modes is debated (Schroeter et al., 2017), and it is becoming increasingly argued that sea ice variability trends especially in the Atlantic Sector are primarily driven by local weather events rather than larger scale atmospheric features (Kwok et al., 2017; Matear et al., 2015). This is of particular importance in the Southern Ocean, as it hosts some of the most energetic storms on the planet. It has been shown that intense polar cyclones can reshape the underlying MIZ and pack ice, as the strong winds induce synoptic scale rotation into the ice floes while carrying warm, moist air along their trajectory (Vichi et al., 2019; Wang et al., 2014). As extratropical cyclones shift poleward and polar storms intensify (Fyfe, 2003; Zhang et al., 2004), it therefore necessary to consider the effect that local weather systems have on ice dynamics to better understand the mechanisms by which longer term sea ice variability is driven.

This study proposes a method for the quantification and detection of rotational features in Antarctic sea ice at daily timescales. The aim is to use it as a potential climate index with which interannual dynamical trends can be analysed. This study does not attempt to identify the mechanisms injecting rotational momentum into the ice field, but rather to automate the detection of these features using currently available ice motion vector products. Several ice motion products are operationally available, all of which undergo unique processing chains. It was therefore necessary to compare the relative performance between different products first. As the aim of this study is to capture dynamical features in the Antarctic sea ice in response to weather events, the highest available temporal resolution from ice motion products were used (48 h). This method revealed a large discrepancy in cyclonic features between sea ice drift products, and thus any further trend analysis would vary depending on the choice of product used. We will also show that the processing chain used in the development of the multi-sensor merged ice motion product can induce additional rotational energy into the resultant vector field.

Data

Four different products from the EUMETSAT OSI SAF low resolution sea ice drift product range (or OSI-405-c) were used in this analysis: the multi-sensor merged, AMSR-2, ASCAT and the SSMI/S range, all covering the overlapping period 2015-2020. The OSI-405-c processing starts from daily maps of brightness temperature, aggregated from swath data measured from the mentioned sensors, namely: the AMSR-2 on JAXA platform GCOM-W1; the SSMI on DMSP platform F15, the SSMIS on DMSP platforms F17 and F18 and the backscatter data from the ASCAT sensor on EUMETSAT platform MetOp-A. Motion vectors derived from the SSMI/S instrument range were stacked sequentially to produce a continuous dataset of measurements between 2015-2020. A Laplacian filter is applied to these daily maps to enhance specific ice features in the image and an ice-edge mask (OSI-402-c product) is also applied. Displacement vectors are then computed from two daily images 48 h apart using a feature tracking method. The multi-sensor merged product treats missing data by means of a two-step process, firstly by using a weighted average of all valid single-sensor data at a particular grid point, and secondly by interpolating surrounding vectors for grid points where no data is available from any single-sensor product. The OSI-405-c

https://doi.org/10.5194/tc-2021-144
Preprint. Discussion started: 25 May 2021

product range was used because its spatial coverage spans over the entire Antarctic sea ice landscape with a comparably intermediate temporal resolution of 48 h, although the 62.5 km spatial resolution is large. The OSI-405-c processing chain uses the Continuous Maximum Cross Correlation method, which includes an additional processing step on the traditionally used Maximum Cross Correlation method. This additional step reduces the high level of quantization noise that typically hinders displacement vector retrieval over short time periods (Lavergne et al., 2010). Antarctic OSI-405-c motion vectors are mapped onto a polar stereographic projection and are available from April 2013 to present at near real-time - making it a good candidate for trend analyses and operational use. Further information on the OSI-405-c product processing chain can be found in Lavergne et al. (2010). Only the 2015-2020 period of complete overlap between the different products is used in this paper.

3 Methodology

Sea ice vorticity features were identified using the multi-sensor merged, AMSR-2, ASCAT and SSMI/S products. The first step in identifying the sea ice vorticity features involves defining the regional domain of interest (D) on the polar stereographic grid, which will serve as the area in which the algorithm will search for features. The domain used in this analysis is the Atlantic Sector of the Southern Ocean, spanning the ice-covered region between 65° W and 10° E from April to November 2015-2020. The months of December - March are excluded as there is not sufficient ice cover during these months to estimate drift vectors. The relative vorticity field:

$$\zeta = \frac{\delta v}{\delta x} - \frac{\delta u}{\delta y}, \quad (1)$$

is computed using the ice drift products, where u and v are the horizontal and vertical components of the drift respectively, and x and y are the horizontal and vertical distance between adjacent points on the 62.5 km spatial resolution grid. Following this, virtual subdomains D_r of radius r are generated around every grid point in D. The mean vorticity of all data points included within every subdomain D_r is computed. For every 48 hours dataset, the subdomains which yield the highest and lowest mean vorticity are classified as the most intense anticyclonic and cyclonic features, respectively. A minimum pixel validity threshold of T is required by every subdomain D_r to ensure that classified features have an adequate number of valid data points, thus reducing the algorithm's susceptibility to selecting small regions of intense vorticity at the ice edge or coastline. Any subdomain area with a mean vorticity of zero is ignored. This process is repeated independently per product with varying r (500, 450 and 400 km) and T (90, 85 and 80 %) parameter values.

4 Results

Figure 1 shows the interannual intensity distribution of cyclonic vorticity features identified by the algorithm described in Methods from 2015 - 2020. Figure 2 shows the interannual distribution of the intensity of anticyclonic vorticity features over the same period. The box-and-whisker rectangles indicate the interquartile range (IQR), with the median line separating the

https://doi.org/10.5194/tc-2021-144
Preprint. Discussion started: 25 May 2021

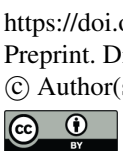

125 upper (Q3) and lower (Q1) quartiles. Outlier vorticity features are shown as dots and represent features which exceed the upper bound ($> Q3 + 1.5 \times IQR$) or lower bound ($< Q1 - 1.5 \times IQR$).

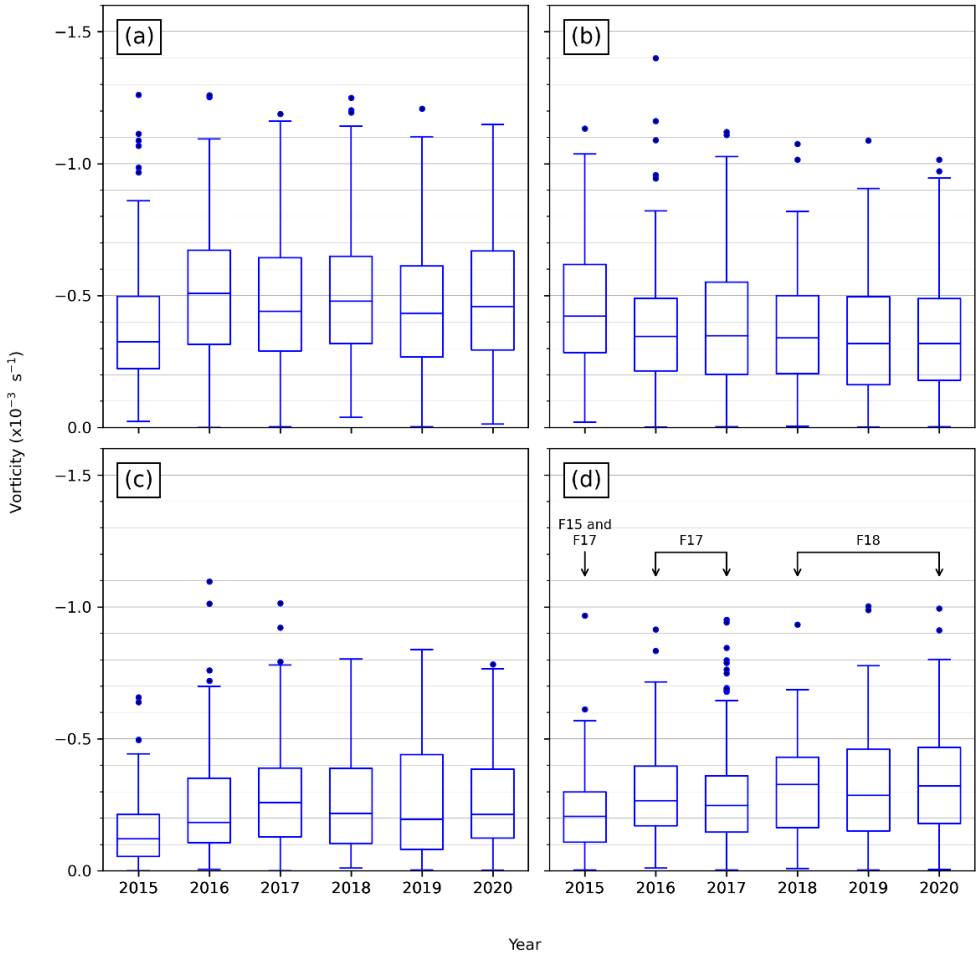

Figure 1: The interannual distribution of the intensity of cyclonic vorticity features identified by the algorithm using OSI-SAF ice motion vector products from products (a) Multi-sensor merged, (b) AMSR-2, (c) ASCAT and (d) SSMI/S
130 **range. Note that the negative y axis is reverted to compare with Fig. 2.**

There was no obvious agreeable pattern in the distribution of cyclonic vorticity across the four ice motion products (Fig. 1). The smallest spread of cyclone features from the merged ice motion appeared in 2015 (Fig. 1a), followed by an initial increase in spread in 2016 and then a relatively unchanging spread from 2016 - 2020. This increased spread from 2015 to 2016 was
135 also detected using the ASCAT (Fig. 1c) and SSMI/S (Fig. 1d) products, but unlike with the merged product, the increasing trend continued beyond 2016 for the ASCAT and SSMI/S products. The ASCAT product showed a consistently increasing spread from 2015 - 2019, followed by a slight decrease in 2020. This decrease in spread in 2020 was not detected by any of the other three products. The AMSR-2 product showed the most unique pattern of distribution with no obvious trend seen, but

https://doi.org/10.5194/tc-2021-144
Preprint. Discussion started: 25 May 2021

instead high levels of interannual variability is evident (Fig. 1b). While outlier cyclonic features were detected in most years, it is apparent that the years 2015, 2016 and 2017 shared a disproportionately large number of these outlier features across all four products, the largest of which being detected in 2016 using the AMSR-2 derived product.

Unlike that of cyclonic features, the distribution of anticyclonic vorticity features is far more agreeable and highlights the much-reduced intensity of this circulation in the domain. While no obvious interannual trend is apparent, the merged (Fig. 2a), AMSR-2 (Fig. 2b) and SSMI/S (Fig. 2c) products detected a similar spread of features. Alternating years of low and high spread are evident using these three products, with similar enhancement of the intensity especially in 2017 and 2019. The ASCAT product detected a similar pattern of interannual spread (Fig. 2c), but at relatively low intensities compared to the other three products.

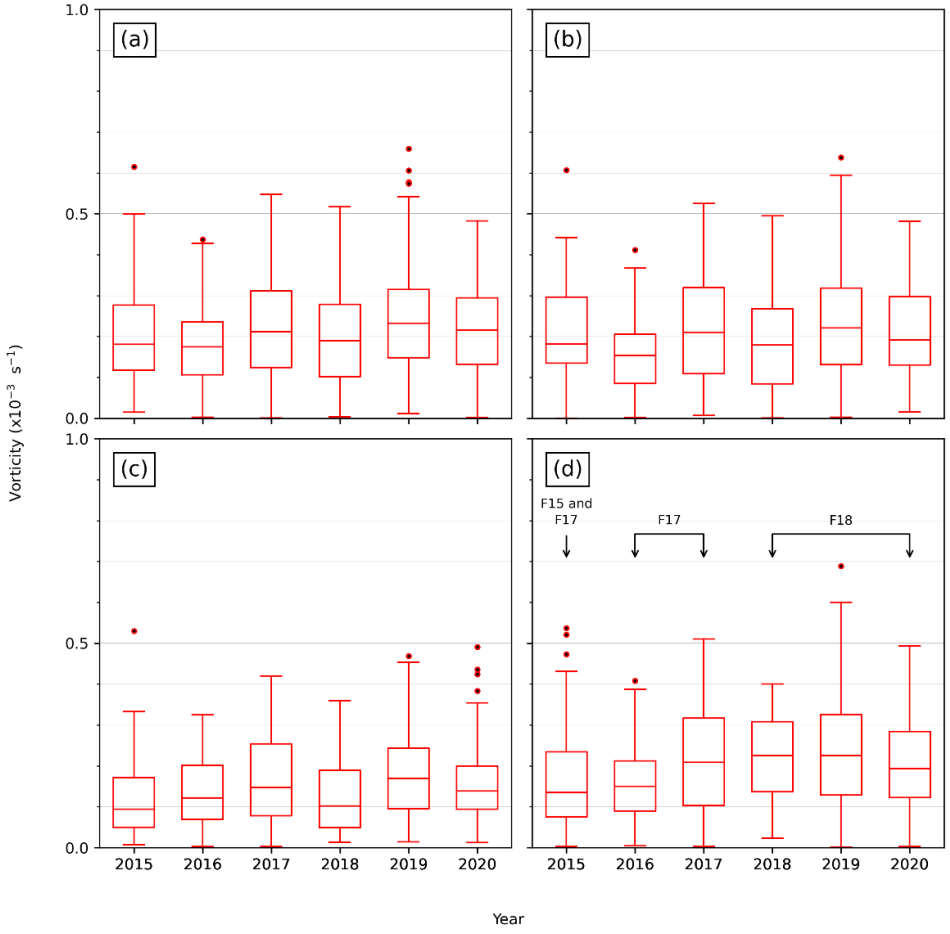

Figure 2: The interannual distribution of the intensity of cyclonic vorticity features identified by the algorithm using OSI-SAF ice motion vector products from instruments (a) Multi-sensor merged, (b) AMSR-2, (c) ASCAT and (d) SSMI/S range. Note that the y axis range is smaller than in Fig. 1.

https://doi.org/10.5194/tc-2021-144
Preprint. Discussion started: 25 May 2021

The merged product detected both the greatest mean and median vorticity magnitudes for both cyclonic features (mean = -0.466 $\times 10^{-3}$ s^{-1}; median = -0.433 $\times 10^{-3}$ s^{-1}) and for anticyclonic features (mean = 0.210 $\times 10^{-3}$ s^{-1}; median = 0.198$\times 10^{-3}$ s^{-1}). This indicates that the merged product detected more rotation in the ice field than any other product. Conversely, the ASCAT product showed both the smallest mean and median magnitudes for both cyclonic features (mean = -0.245 $\times 10^{-3}$ s^{-1}, median = -0.186 $\times 10^{-3}$ s^{-1}) and for anticyclonic features (mean = 0.145 $\times 10^{-3}$ s^{-1}, median = 0.133 $\times 10^{-3}$ s^{-1}). A difference between the cyclonic and anticyclonic feature intensity is clear, the greatest of which is detected using the merged product where the cyclonic feature intensity is approximately 2.2 times greater than that of its anticyclonic features. This difference is also detected using the three other products - although to a lesser extent - with the SSMI/S product detecting the smallest difference factor of approximately 1.5.

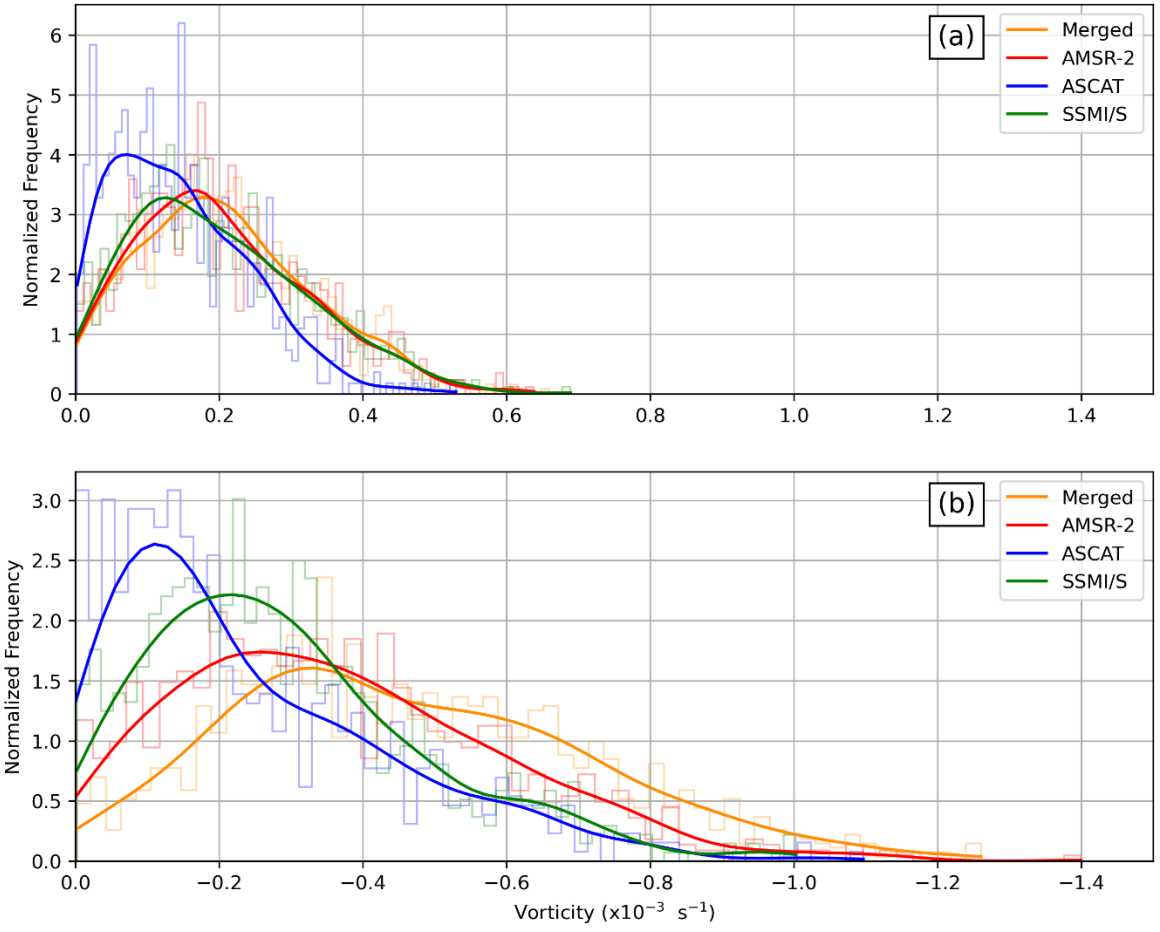

Figure 3: The normalized frequency distribution of (a) anticyclonic vorticity features and (b) cyclonic vorticity features (note the reverted x axis for comparison). Lighter shaded lines show a stepped histogram of 60 bins, while the darker shaded line represents a kernel-density estimate using Gaussian kernels.

https://doi.org/10.5194/tc-2021-144
Preprint. Discussion started: 25 May 2021

The difference in spread and intensity between cyclonic and anticyclonic features is evident in Fig. 3, where the empirical, normalized Gaussian curve estimated over the study period shows the relative frequency of detection of high and low intensity circulation features. The ASCAT product detects a much larger frequency of low magnitude features for both anticyclonic (IQR = 0.143; σ = 0.10) and cyclonic (IQR = 0.259; σ = 0.20) features (Fig. 3). Anticyclonic feature spread detected using the multi-sensor merged (IQR = 0.169; σ = 0.12), AMSR-2 (IQR = 0.166; σ = 0.12) and SSMI/S (IQR = 0.173; σ = 0.12) derived products are more in agreement. Conversely, substantial variation in cyclonic feature spread between products is seen in Fig. 3b. Here, the merged product generated the largest intensity and tail (IQR = 0.357; σ = 0.25), indicating that a disproportionately high frequency of intermediate-to-high intensity features were detected using the merged product. The AMSR-2 product generated the second largest tail (IQR = 0.309; σ = 0.22). While the ASCAT (IQR = 0.259; σ = 0.20) and SSMI/S (IQR = 0.240; σ = 0.19) products showed a similar spread of cyclonic features, the features detected by the SSMI/S products were of a larger intensity, peaking at ~ -0.2 s^{-1}. All permutations of varying parameter values radius r and threshold T produced similar results (not shown), indicating that the presented difference between the products is robust to the choice of the free parameters.

5 Discussion and Conclusions

Analysis of cyclonic circulation features computed from remote sensing sea-ice drift data during 2015 – 2020 showed a large discrepancy between products, both in the annual distributions (Fig. 1) and the intensity of features detected (Fig. 3b). Despite the short overlapping period, three of the ice motion products (merged, ASCAT and SSMI/S) indicated a substantial increase in cyclonic vorticity from 2015 to 2016, which aligns well with the hypotheses of increased storminess and sudden sea-ice decrease experienced during these years (Parkinson, 2019; Turner et al., 2017). However, two other products (ASCAT and SSMI/S) pointed towards an overall increasing trend throughout the period (Fig. 1) and the AMSR-2 product indicated alternating years of high and low spread, a pattern not seen using any other product. In contrast, the analysis of anticyclonic circulation features across products was more in agreement. Despite the ASCAT product showing a skewed distribution towards low intensity features (a pattern also observed in the cyclone distribution, Fig. 3), the interannual spread between products was similar (Fig. 2). This agreement between products therefore improves the confidence of these results for detecting anticyclonic feature variability and trend analysis, however no obvious trend is apparent over the 2015-2020 period.

Detected cyclonic features were measured to be between 1.5-2.2 times more intense than that of anticyclonic features, indicating an overall negative skew in the vorticity distribution which is independent of product choice. Antarctic sea ice in the Atlantic Sector is therefore shown not to be in rotational balance at daily timescales, supporting arguments that local weather events could inject synoptic scale cyclonic momentum into the ice. Interestingly, results using the merged product detected a disproportionately large frequency of high intensity features relative to the other products (Fig. 3b). Since the merged

https://doi.org/10.5194/tc-2021-144
Preprint. Discussion started: 25 May 2021

product is computed using a combination of the other sensors, it would be expected that this product would produce intermediate-level results, acting much like a balance between the extremes of its components. Instead, more rotation in the ice was detected than any other product, suggesting that the merging processing chain could add additional energy into the resultant ice drift vectors. The disproportionately high frequency of low intensity features detected using the ASCAT is potentially linked to the spatial distribution of detected features, where most features were detected in the Eastern Weddell Sea (not shown). This could be a result of the patchiness of available data using the ASCAT sensor, whereby features meeting the valid-pixel threshold were only consistently retrievable in the Eastern Weddell Sea. However, repetitions of this processing with adjusted valid-pixel threshold values (80-90 %) and synoptic feature radius values (400-500 km) produced similar results, suggesting that the algorithm is not particularly sensitive to the choice of these parameters.

The intention of this investigation was to develop a new method by which to detect sea ice drift trends and variability, and more specifically, to establish a measure of variability in synoptic scale rotation in the Southern Ocean sea ice. While anticyclonic feature detection between products showed good agreement, a large interannual discrepancy in cyclonic feature detection between products is evident. As it is intuitive that Atlantic weather events will drive cyclonic drift in the underlying ice field, it is therefore necessary to better understand these cyclonic feature detection discrepancies between products before attempting to understand the effect of atmospheric cyclones on sea ice. Additionally, it was also found that the processing chain used in the development of the multi-sensor merged ice drift product can induce additional rotational energy into the resultant vector field. These results indicate that any further analysis of drift variability and trends would vary greatly depending on the choice of product, thus diminishing our confidence in the results. This study therefore concludes that the discrepancy between products is hindering our ability to quantify interannual cyclonic drift variability, and that a better understanding of these discrepancies is required before this variability can be confidently used as an essential climate variable.

Acknowledgements

This work has received funding from the National Research Foundation of South Africa (South African National Antarctic Programme, Project No. 118745).

Data availability

The OSI-405-c product is available at http://www.osi-saf.org/?q=content/global-low-resolution-sea-ice-drift-c. The python scripts to compute the cyclonic and anticyclonic circulation are available at: https://github.com/waynedejagerUCT/publications/blob/a224a291d2664d2ffcdc7899a0e5954360a222c4/VorticityFeatureSearch_v001

https://doi.org/10.5194/tc-2021-144
Preprint. Discussion started: 25 May 2021

230 **References**

Comiso, J. C. and Zwally, H. J.: Concentration gradients and growth/decay characteristics of the seasonal sea ice cover., J. Geophys. Res., doi:10.1029/JC089iC05p08081, 1984.

Feltham, D. L.: Sea Ice Rheology, Annu. Rev. Fluid Mech., 40(1), 91–112, doi:10.1146/annurev.fluid.40.111406.102151, 2008.

235 Fyfe, J. C.: Extratropical Southern Hemisphere Cyclones: Harbingers of Climate Change?, J. Clim., 16(17), 2802–2805, doi:10.1175/1520-0442(2003)016<2802:ESHCHO>2.0.CO;2, 2003.

Goosse, H., Lefebvre, W., de Montety, A., Crespin, E. and Orsi, A. H.: Consistent past half-century trends in the atmosphere, the sea ice and the ocean at high southern latitudes, Clim. Dyn., 33(7–8), 999–1016, doi:10.1007/s00382-008-0500-9, 2009.

Holland, P. R. and Kwok, R.: Wind-driven trends in Antarctic sea-ice drift, Nat. Geosci., 5(12), 872–875,
240 doi:10.1038/ngeo1627, 2012.

Kohout, A. L., Williams, M. J. M., Dean, S. M. and Meylan, M. H.: Storm-induced sea-ice breakup and the implications for ice extent, Nature, doi:10.1038/nature13262, 2014.

Kwok, R., Pang, S. S. and Kacimi, S.: Sea ice drift in the Southern Ocean: Regional patterns, variability, and trends, edited by J. W. Deming and E. C. Carmack, Elem. Sci. Anthr., 5, doi:10.1525/elementa.226, 2017.

245 Lavergne, T., Eastwood, S., Teffah, Z., Schyberg, H. and Breivik, L.-A.: Sea ice motion from low-resolution satellite sensors: An alternative method and its validation in the Arctic, J. Geophys. Res., 115(C10), C10032, doi:10.1029/2009JC005958, 2010.

Martinson, D. G. and Iannuzzi, R. A.: Antarctic Ocean-Ice Interaction: Implications from Ocean Bulk Property Distributions in the Weddell Gyre., 2013.

Matear, R. J., O'Kane, T. J., Risbey, J. S. and Chamberlain, M.: Sources of heterogeneous variability and trends in Antarctic
250 sea-ice, Nat. Commun., 6(1), 8656, doi:10.1038/ncomms9656, 2015.

Mayewski, P. A., Meredith, M. P., Summerhayes, C. P., Turner, J., Worby, A., Barrett, P. J., Casassa, G., Bertler, N. A. N., Bracegirdle, T., Naveira Garabato, A. C., Bromwich, D., Campbell, H., Hamilton, G. S., Lyons, W. B., Maasch, K. A., Aoki, S., Xiao, C. and van Ommen, T.: State of the Antarctic and Southern Ocean climate system, Rev. Geophys., 47(1), RG1003, doi:10.1029/2007RG000231, 2009.

255 McPhee, M. G., Maykut, G. A. and Morison, J. H.: Dynamics and thermodynamics of the ice/upper ocean system in the marginal ice zone of the Greenland Sea, J. Geophys. Res., 92(C7), 7017, doi:10.1029/JC092iC07p07017, 1987.

Notz, D. and Community, S.: Arctic Sea Ice in CMIP6, Geophys. Res. Lett., 47(10), doi:10.1029/2019GL086749, 2020.

Parkinson, C. L.: A 40-y record reveals gradual Antarctic sea ice increases followed by decreases at rates far exceeding the rates seen in the Arctic, Proc. Natl. Acad. Sci. U. S. A., doi:10.1073/pnas.1906556116, 2019.

260 Pezza, A. B., Rashid, H. A. and Simmonds, I.: Climate links and recent extremes in antarctic sea ice, high-latitude cyclones, Southern Annular Mode and ENSO, Clim. Dyn., 38(1–2), 57–73, doi:10.1007/s00382-011-1044-y, 2012.

Schroeter, S., Hobbs, W. and Bindoff, N. L.: Interactions between Antarctic sea ice and large-scale atmospheric modes in

https://doi.org/10.5194/tc-2021-144
Preprint. Discussion started: 25 May 2021

CMIP5 models, Cryosph., 11(2), 789–803, doi:10.5194/tc-11-789-2017, 2017.

Stevens, R. P. and Heil, P.: The interplay of dynamic and thermodynamic processes in driving the ice-edge location in the Southern Ocean, Ann. Glaciol., 52(57), 27–34, doi:10.3189/172756411795931642, 2011.

Thompson, D. W. J.: Interpretation of Recent Southern Hemisphere Climate Change, Science (80-.)., 296(5569), 895–899, doi:10.1126/science.1069270, 2002.

Turner, J., Scott Hosking, J., Marshall, G. J., Phillips, T. and Bracegirdle, T. J.: Antarctic sea ice increase consistent with intrinsic variability of the Amundsen sea low, Clim. Dyn., doi:10.1007/s00382-015-2708-9, 2016.

Turner, J., Phillips, T., Marshall, G. J., Hosking, J. S., Pope, J. O., Bracegirdle, T. J. and Deb, P.: Unprecedented springtime retreat of Antarctic sea ice in 2016, Geophys. Res. Lett., 44(13), 6868–6875, doi:10.1002/2017GL073656, 2017.

Uotila, P., Vihma, T., Pezza, A. B., Simmonds, I., Keay, K. and Lynch, A. H.: Relationships between Antarctic cyclones and surface conditions as derived from high-resolution numerical weather prediction data, J. Geophys. Res. Atmos., doi:10.1029/2010JD015358, 2011.

Vichi, M., Eayrs, C., Alberello, A., Bekker, A., Bennetts, L., Holland, D., Jong, E., Joubert, W., MacHutchon, K., Messori, G., Mojica, J. F., Onorato, M., Saunders, C., Skatulla, S. and Toffoli, A.: Effects of an Explosive Polar Cyclone Crossing the Antarctic Marginal Ice Zone, Geophys. Res. Lett., 46(11), 5948–5958, doi:10.1029/2019GL082457, 2019.

Vihma, T., Pirazzini, R., Fer, I., Renfrew, I. A., Sedlar, J., Tjernström, M., Lüpkes, C., Nygård, T., Notz, D., Weiss, J., Marsan, D., Cheng, B., Birnbaum, G., Gerland, S., Chechin, D. and Gascard, J. C.: Advances in understanding and parameterization of small-scale physical processes in the marine Arctic climate system: a review, Atmos. Chem. Phys., 14(17), 9403–9450, doi:10.5194/acp-14-9403-2014, 2014.

Wang, Z., Turner, J., Sun, B., Li, B. and Liu, C.: Cyclone-induced rapid creation of extreme Antarctic sea ice conditions, Sci. Rep., doi:10.1038/srep05317, 2014.

Yuan, X.: ENSO-related impacts on Antarctic sea ice: A synthesis of phenomenon and mechanisms, Antarct. Sci., doi:10.1017/S0954102004002238, 2004.

Zhang, X., Walsh, J. E., Zhang, J., Bhatt, U. S. and Ikeda, M.: Climatology and Interannual Variability of Arctic Cyclone Activity: 1948–2002, J. Clim., 17(12), 2300–2317, doi:10.1175/1520-0442(2004)017<2300:CAIVOA>2.0.CO;2, 2004.